RICE UNVERSITY

A MONTE CARLO STUDY OF HIGH TRANSVERSE ENERGY TRIGGERS IN PP COLLISIONS AT P_{lab}=400 Gev/c.

by

CHARLES JOSEPH NAUDET

A THESIS SUBMITTED
IN PARTIAL FULLFILLIMENT OF THE
REQUIREMENTS FOR THE DEGREE

MASTER OF ARTS

APPROVED, THESIS COMMITTEE

Hannu E. Mietinen, Assistant Professor of Physics
CHAIRMAN

Ian Duck, Professor of Physics

James Hannon, Professor of Physics

HOUSTON, TEXAS
APRIL, 1983

FERMILAB LIBRARY

ABSTRACT

A Monte Carlo Study Of High Transverse Energy Triggers In pp Collisions At P = 400 Gev/c.

by

Charles J. Naudet Jr.

We have studied the properties of typical inelastic final states in pp collisions at p_{lab} =400 Gev/c under triggering conditions similar to those used in actual jet experiments. The events were generated by a Monte Carlo method which employed experimentally observed multiplicity and inclusive momentum distributions and constrained all the events to conserve momentum and energy. We find that a requirement of high transverse energy in a given solid angle selects mostly very high multiplicity events. Some experimentally observed momentum correlations seem to be of kinematical orgin and the triggered events have a similar transverse energy spectrum, but a less coplanar event structure than what is observed in experimental data.

Acknowledgments

It is my pleasure to thank all of my friends and colleagues at T.W. Bonner laboratory and Rice University. In particular I would like to thank my advisor Professor Hannu E. Mietinen, for without his quidence,criticism and patience this thesis may never have been completed. I would also like to show my appreciation to Professor Jabus B. Roberts whom taught me both experimental physics and rugby. A special thanks goes to a fellow comrade in arms Ken Johns, whose friendship and unrelenting drive made the unending months on the experimental sites a bit easiler to handle.

Finally; I wish to thank my parents,brothers and sisters for all their invaluable support and encouragement throughout my academic career.

TABLE OF CONTENTS

	page
ABSTRACT	i
Acknowledgments	ii
LIST OF FIGURES AND TABLES	iv
CHAPTER I: INTRODUCTION	1
CHAPTER II: GENERATION OF LOW TRANSVERSE MOMENTUM EVENTS	6
A. Multiplicity and Composition	8
B.Conservation of Energy and Momemtum for each Event	18
CHAPTER III: STUDY OF EVENTS SATISFYING A JET TRIGGER	28
A. Single and many Particle Triggers	28
B. Triggering with a Calorimeter	38
CHAPTER IV: CONCLUSIONS	51
REFERENCES	53

LIST OF FIGURES AND TABLES

		page
Flowchart	Program Logic	6
Fig.A-1	Charged Multiplicity Distribution	9
Fig.A-2	Multiplicity Dependence of the Pion	15
Fig.A-3	Multiplicity Dependence of the Kaon	16
Fig.A-4	Total Multiplicity Distribution	17
Fig.A-5	Proton Transverse Momemtum Distribution	20
Fig.A-6	Pion Transverse Momentum Distribution	21
Fig.A-7	Kaon Transverse Momemtum Distribution	22
Fig.A-8	Proton Rapidity Distribution	25
Fig.A-9	Pion Rapidity Distribution	26
Fig.A-10	Kaon Rapidity Distribution	27
Table A1	Average Charged Multiplicities	10
Table A2	Transverse Momentum Cross Sections	10
Fig.B-1	Triggered Total Multiplicity Distribution	30
Fig.B-2	Scatterplot of Multiplicity and Pt	31
Fig.B-3	Planarity Distributions	33
Fig.B-4	Scatterplot of Multiplicity and Planarity	34
Fig.B-5	Delta Phi Distributions	36
Fig.B-6	Away Side Transverse Momentum Distributions	37
Fig.B-7	Away Side Rapidity Distributions	39
Fig.B-8	Ex609 Experimental Calorimeter	40

Fig.B-9 Calorimeter Trigggers 42

Fig.B-10 Global Trigger Multiplicity Distributions 43

Fig.B-11 Global Triggered Planarity Distributions 44

Fig.B-12 Global Planarity Dependence on Multiplicity 45

Fig.B-13 Transverse Energy Distributions 47

Fig.B-14 Single Arm Pt Balancing 49

CHAPTER 1

INTRODUCTION

Over the last several years,deep inelastic hadron-hadron scattering has been quite successfully interpreted by parton models, where it is assumed that the underlying process is incoherent scattering of point-like hadron constituents. According to the hard-scattering parton model, two partons, one from each incident proton, experience a two-body collision and then independently fragment to produce jets. Jets are groups of final state hadrons scattered into a small fraction of the available solid angle. The remaining partons of the interaction produce the beam and target jet and are responsible for most of the low transverse momemtum secondaries (mostly pions).

Past experiments,such as those at the CERN Intersecting Storage Rings (ISR) and at Fermilab, have observed an enhancement of particle density in the region of phase space surrounding large transverse momentum final state hadrons. Strong correlations have been found in transverse momentum,rapidity and azimuth. Experiment E609 [18] at Fermilab was performed to study these phenomena in more detail

in the total centre-of-mass energy range $\sqrt{s}$ =19.8 to 27.4 gev. The goal of this experiment was to trigger on jets using a segmented calorimeter, and to study the frequency and structure of jet-like events in order to extract the hard scattering cross sections.

One difficulty in interpreting the results of jet experiments is that in general the jet fragments are not clearly separated from other hadrons in the event. As a result, fluctuations in "ordinary" low p_t events can sometimes mimic true jet-like events. The clarity of true jet events is further eroded by the experimental difficulties in triggering on groups of hadrons. It is therefore of importance to study ordinary low p_t events carefully and to examine under what conditions they might appear to be jet-like.

The objective of this study,using a Monte Carlo method,was to generate low p_t final states of pp interactions, then to impose various jet-finding triggers and study the accepted events. A comparison of these "jet events" with the normal events will be made along with an examination of the kinematic correlations. Eventually, after the E609 data is properly reduced, a direct comparison will be made with the actual data.

Chapter 2 starts with a brief description of the Monte Carlo program used and a discussion of the important features of the simulation. Next we discuss the creation of the final states with the correct multiplicity distributions, and explain how the final state hadrons ($p, \bar{p}$, k+, k-, pi+, pi-, pi0, n, k0/k0bar) are randomly put into an event at a given multiplicity to produce the correct average composition, while simultaneously conserving baryon number, strangness, and charge. Then we explain how the hadrons are given their transverse momentum (p_t), rapidity, and azimthal angle (ø) distributions and how the events are forced to conserve energy and momentum. Illustrations and a discussion are given on how this process creates a correlation between the p_t and the phi variables in an event. The final section in Chapter 2 is a summary of the event generation method with comments concerning the accuracy and limitations of this simulation.

Application of basic jet-finding triggers to the generated events is studied in Chapter 3. We first describe our single and many particle triggers and define some useful parameters such as planarity. Then we study the effects of triggering on multiplicity, p_t and ø and we compare normal events to the "jet events". Finally we elaborate on the effect of triggering with a calorimeter in the laboratory

frame and on the transverse momentum balancing for various trigger arrangements.

The conclusions are summarized in the final chapter.

CHAPTER 2

GENERATION OF LOW TRANSVERSE MOMENTUM EVENTS

This chapter deals with the Monte Carlo generation of low transverse momentum events. The fortran program used is outlined in Flowchart 1 and the important characteristics are listed below.

1) The charged and total multiplicity distributions agree with the experimental data.

2) Final state particles considered are the proton,antiproton,neutron, charged kaons and pions,and the neutral kaon and pion.

3) The average particle composition is in agreement with the data.

4) Baryon number,Charge,Strangeness,Energy and Momentum are forced to be conserved for every event.

5) The p_t,rapidity and ø distributions are all forced to agree with the experimental inclusive distributions.

6) The leading particle effect is taken into account.

7) There are no resonances and no other dynamic correlations in the final state.

The remaining portion of this chapter describes the methods used to produce the above features.

FLOWCHART 1. This figure illustrates the program logic used in the production of the phase space Monte Carlo events. A brief explanation of the various routines used is given below.

Setup: Reads in the initialization data and sets up histogram routines.

Genchr: Calculates several kinematic variables and the percentage of events to be produced at each multiplicity.

Genpi: The number of particle types ($p, \bar{p}, k^+, k^-, \pi^+, \pi^-, \pi 0, n, k0/k0bar$) at each multiplicity is computed.

Cutoff-Intgra-Func: These subroutines integrate the parameterization of the p_t distribution for each particle type, which will be used in the generation of the p_t for the particles.

Main Program: Besides calling all the subroutines, the main program takes the calculated composition at any multiplicity and distributes all the hadrons ramdomly amoung all the events, conserving Baryon number, strangeness, and charge simultaneously.

Rnmxx-Rpdist: Creates a random number distribution.

Genrap: Using cutoff,rpdist and rnmxx the p_t and rapidity are generated for each particle while conserving energy and momemtum.

Calevt-Myhist: Calculates an assortment of Kinematic variables for each event and histgrams chosen quanities.

Tpaml1: Writes to tape the important information for each correctly produced event.

FLOWCHART

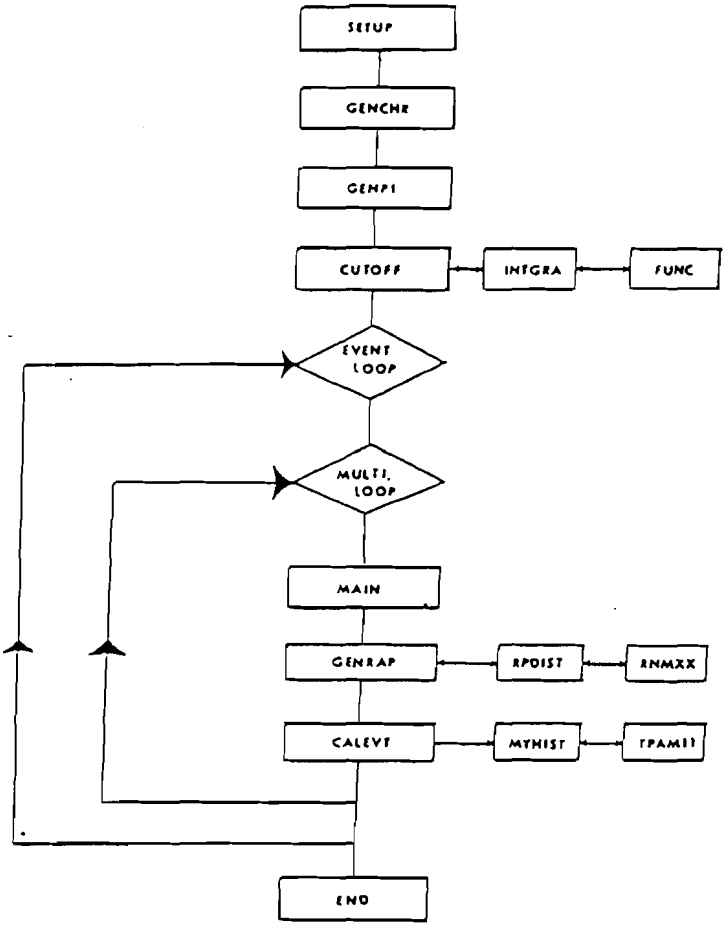
SETUP
GENCHR
GENPI
CUTOFF
INTGRA
FUNC
EVENT LOOP
MULTI. LOOP
MAIN
GENRAP
RPDIST
RNMXX
CALEVT
MYHIST
TPAMIT
END

A) Multiplicity and Composition

In the Monte Carlo generation of the pp inelastic final states it is desired that the charged multiplicity distribution agrees with the experimentally observed data. We accomplish this by using a parameterization given by Moller [1],based on the idea of KNO scaling [2]:

$$P(n)=(1/\sigma^{t}_{inel})d\sigma/dn = 2.76\ z^{.886}\exp(-.758z^{1.886})$$

where $z=(n-\alpha)/\langle n-\alpha\rangle$ and for pp collisions $\alpha=.9$ [3]. The charged multiplicity distribution at a given beam momentum is thus uniquely determined by specifying the average charged multiplicity $\langle n\rangle$ at that momentum. A comparison of P(n) with experimental data at $p_{lab}=400$ gev/c is shown in Figure A-1.

Next we must determine the particle composition,i.e. the relative number of various hadrons in the final states. The hadrons considered are $p,\bar{p}$,k^+,k^-,π^+,π^-,n,and k0/k0bar with no distinction made between the k0 and k0bar. No other hadrons are considered,primarily because they quickly decay into the above hadrons or else there inclusive cross sectons are negligible in comparison.

In the course of discussion on the compostion of events we use the following notation:

Figure A-1. This figure shows both the experimentally observed charged multiplicity distribution at P_{lab}=400 gev/c and the distribution obtained from the Phase Space Monte Carlo.

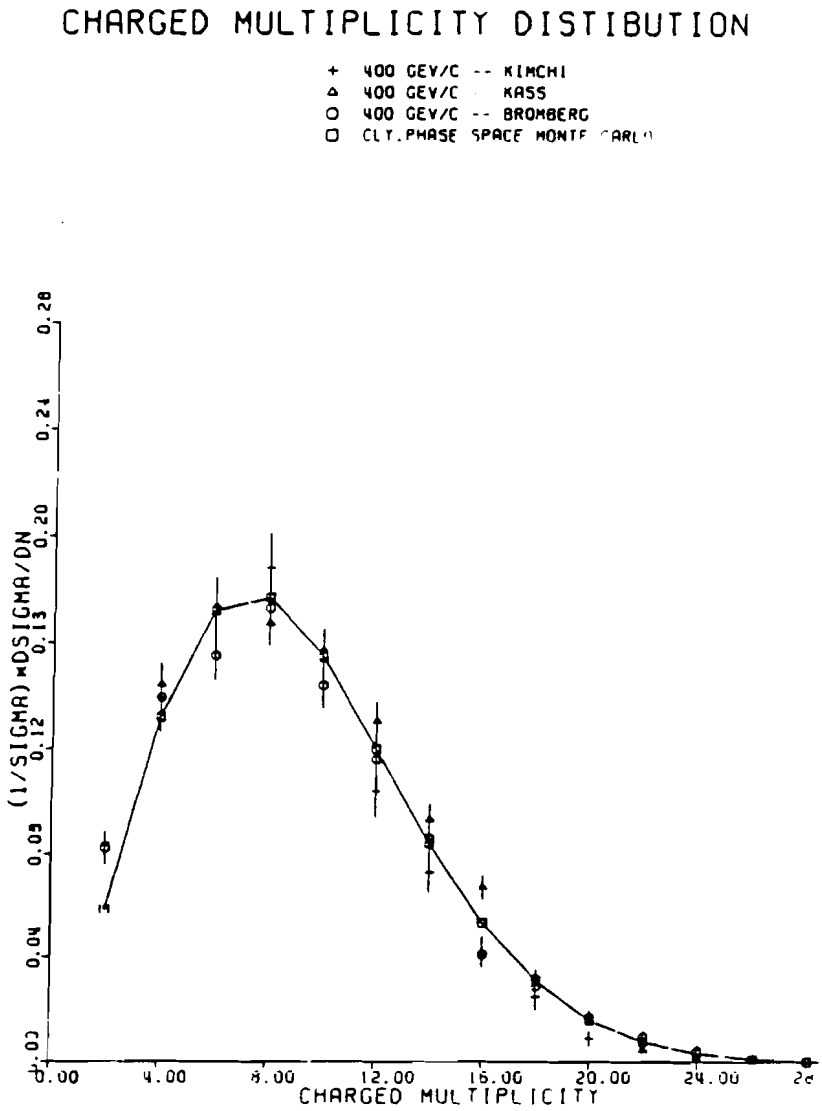

TABLE A-1. The table below shows the average number of the various particle types per event at several different beam momentums.

P_{lab}	$\langle p \rangle$	$\langle p^- \rangle$	$\langle K^+ \rangle$	$\langle K^- \rangle$	$\langle \pi^+ \rangle$	$\langle \pi^- \rangle$	$\langle nch \rangle$/exp
200	1.3	.03	.30	.17	3.25	2.60	7.7/7.68
300	1.3	.04	.35	.21	3.60	3.00	8.5/8.50
400	1.3	.06	.38	.24	3.82	3.20	9.0/8.99

Table A-2. The list below shows the input inclusive transverse momentum distributions used for the final state hadrons produced in the Monte Carlo.

Proton, antiproton, and neutron $\quad \frac{d\sigma}{dp_T} = 11 p_T e^{-12 p_T^2} + 3.26 e^{-3 p_T^2} p_T$

K^+, K^- and $K\emptyset/\overline{K\emptyset}$ $\quad \frac{d\sigma}{dp_T} = \begin{cases} 8.7 p_T \exp(-4.81 p_T^2) & \text{if } p_T < .55 \\ 4.97 p_T \exp(-3.12 p_T^2) & \text{if } p_T \geq .55 \end{cases}$

π^+, π^-, and π^0 $\quad \frac{d\sigma}{dp_T} = 13.38 p_T e^{-14.7 p_T^2} + 3.26 p_T e^{-8.2 p_T^2}$

N_t= total number of events to be produced.

$N_n = N_t P(n)$=number of events to be produced at charged multiplity n,

$\langle x \rangle = (1/\sigma^t_{inel}) \int \frac{d\sigma}{dn}(pp \to 'n'x + anything) dn$= average number of particle type X per event,

$\langle x \rangle_n = \frac{d\sigma}{dn}(pp \to 'n'x + anything) / (\frac{d\sigma}{dn}(pp\text{-}inelastic))$= average number of particle type X per event at a given multplicity n,

$n(x)_n = N_n \langle x \rangle_n$= total number of particle type x at multplicity n,

$m(x)_n$=number of x's actually assigned to an event at multilplity n.

Our method of generating the final states is to calculate the number of hadrons at a given charged multiplicty ($n(x)_n$) and then randomly distribute these hadrons amoung the N_n events. The average number of various particle types per event (i.e.$\langle x \rangle$) is quite well-known experimentally, and is given in Table A-1 which is based on a compilation by Antinucci et.al.[4]. On the other hand, there is very little data on the multiplicity dependence of $\langle x \rangle$ (ie. on $\langle x \rangle_n$), and we must therefore resort to reasonable physical assumptions about this dependence. These assumptions are stated below for each particle type.

:Generation of the Baryons:

We begin by generating the antiprotons, and assume that the ratio of the number of antiprotons to the number of negative hadrons, is independent of multiplicity:

$$\langle\bar{p}\rangle_n/\langle n^-\rangle_n=\langle\bar{p}\rangle/\langle n^-\rangle$$

where n^- is the number of negative particles.† Therfore;

$$\langle\bar{p}\rangle_n=\{\langle\bar{p}\rangle/(\langle k^-\rangle+\langle\pi^-\rangle+\langle\bar{p}\rangle)\}(n/2\ -1)$$

and $n(\bar{p})_n=N_n\langle\bar{p}\rangle_n$. These $n(\bar{p})_n$ antiprotons are then randomly assigned to the N_n final states at multiplicity n.

Since the $\bar{p}$ production is primarily due to $\bar{p}p$ pair production, we generate a "slow" proton for each antiproton. The remaining "fast" protons (leading particles) are produced by assuming that $\langle p\rangle_n=\langle p\rangle$ [7], ie. that the average number of all protons is independent of multiplicity. Therfore;

$$\langle p\text{-fast}\rangle_n=\langle p\rangle-\langle\bar{p}\rangle_n.$$

The $N_n\langle p\text{-fast}\rangle_n$ fast protons are again randomly distributed amoung the N_n events at multiplicity n, with the constraint that no event have more than two fast protons. Finally to conserve the Baryon number we add neutrons, thus,

$$m(n)_n=2-m(p\text{-fast})_n.$$

† $n^-=(n/2)-1$, since $n^++n^-=n$ and $n^+-n^-=2$.

:Generation of Charged Kaons and Pions

For the negative kaons the same assumption is made as for the antiprotons, that is,

$$\langle k^- \rangle_n / \langle n^- \rangle_n = \langle k^- \rangle / \langle n^- \rangle$$

Thus; $\langle k^- \rangle_n = \{\langle k^- \rangle / (\langle k^- \rangle + \langle \pi^- \rangle + \langle \bar{p} \rangle)\}(n/2 - 1)$

and $n(k^-)_n = N_n \langle k^- \rangle_n$.

The number of postive kaons is determined in a similar way, apart from subtracting out the protons (since $\langle p \rangle_n$=constant). Hence,

$$\langle k^+ \rangle_n = \{\langle k^+ \rangle / (\langle k^+ \rangle + \langle \pi^+ \rangle)\}(n/2 - 1 - \langle p \rangle)$$

and $n(k^+)_n = N_n \langle k^+ \rangle_n$. These $n(k^+)_n$ and $n(k^-)_n$ kaons are then randomly distributed among the events with the charge conservation constraints,

$$m(k^+)_n + m(p)_n < (n/2+1) \text{ and } m(k^-)_n + m(\bar{p})_n < (n/2-1).$$

Finally the charged pions are introduced into the final states by simply forcing the conservation of charge. Thus,

$$m(\pi^+)_n = (n/2+1) - m(p)_n - m(k^+)_n$$

$$m(\pi^-)_n = (n/2-1) - m(\bar{p})_n - m(k^-)_n.$$

:Remaining Neutrals:

The average number of neutral pions and kaons as a

function of multiplicity is rather well-known experimentally; at p_{lab}=400 gev/c we use the following parameterizations,[5,6,15,16].

$$\langle \pi^0 \rangle_n = \begin{cases} .65(n/2-1)+2.05 & \text{if } n<20 \\ 7.9 & \text{if } n \geq 20 \end{cases}$$

$$\langle k0/k0bar \rangle_n = \begin{cases} .074(n/2-1)+.156 & \text{if } n<20 \\ .822 & \text{if } n \geq 20 \end{cases}$$

With these parameterizations it is trival to obtain $n(\pi^0)_n$ and $n(k0/k0bar)_n$. These neutral pions and kaons are then added to the final states in a random fashion. The neutral kaons however,are assigned to the final states in such a manner as to conserve strangeness.

After the neutral pions and kaons have been included in the final states the construction of the composition of the events is complete. A comparison of the output from the Monte Carlo to the experimental data on the multiplicity dependence of the average number of neutral kaons and pions is shown in Figures A-2 and A-3 respectively. The total multiplicity distribution is shown in Figure A-4; the average total multiplicity being 15.2.

Figure A-2. The average number of neutral pions for a given multiplicity is shown for both the experimental data and the output from the Phase Monte Carlo.

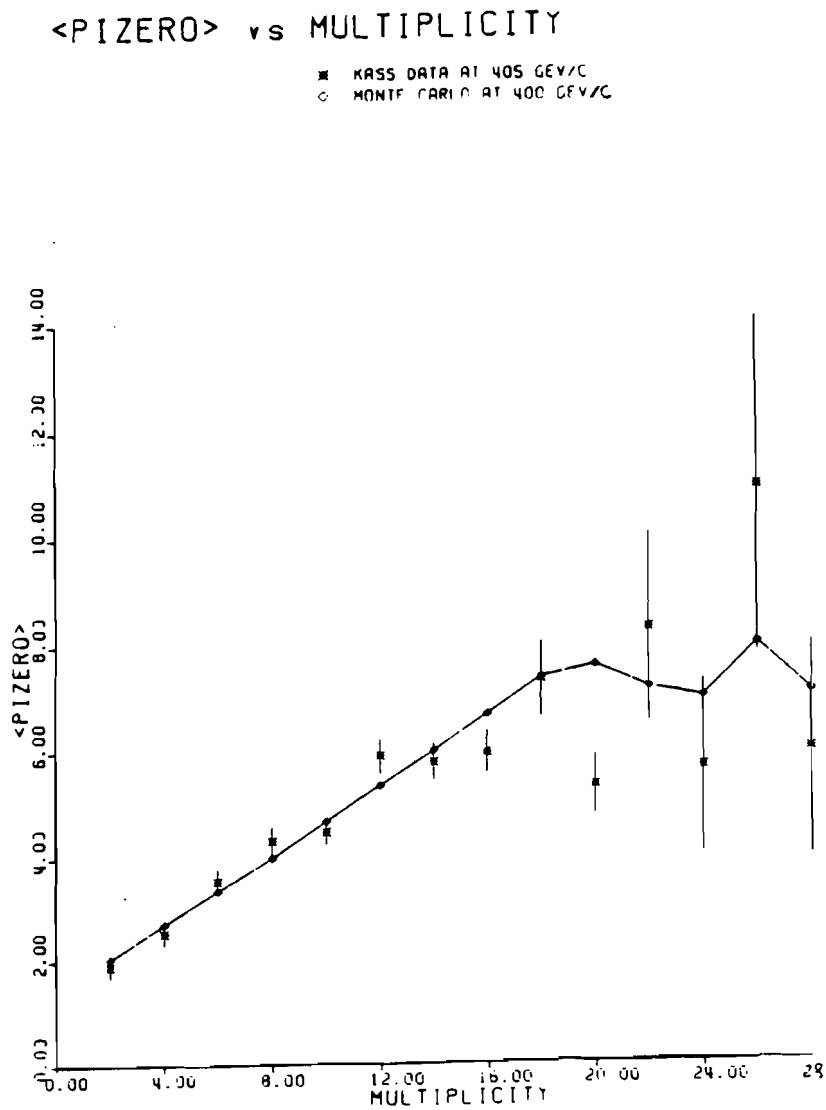

Figure A-3. The average number of neutral kaons for a given multiplicity is shown for both the experimental data and the Phase Space Monte Carlo events.

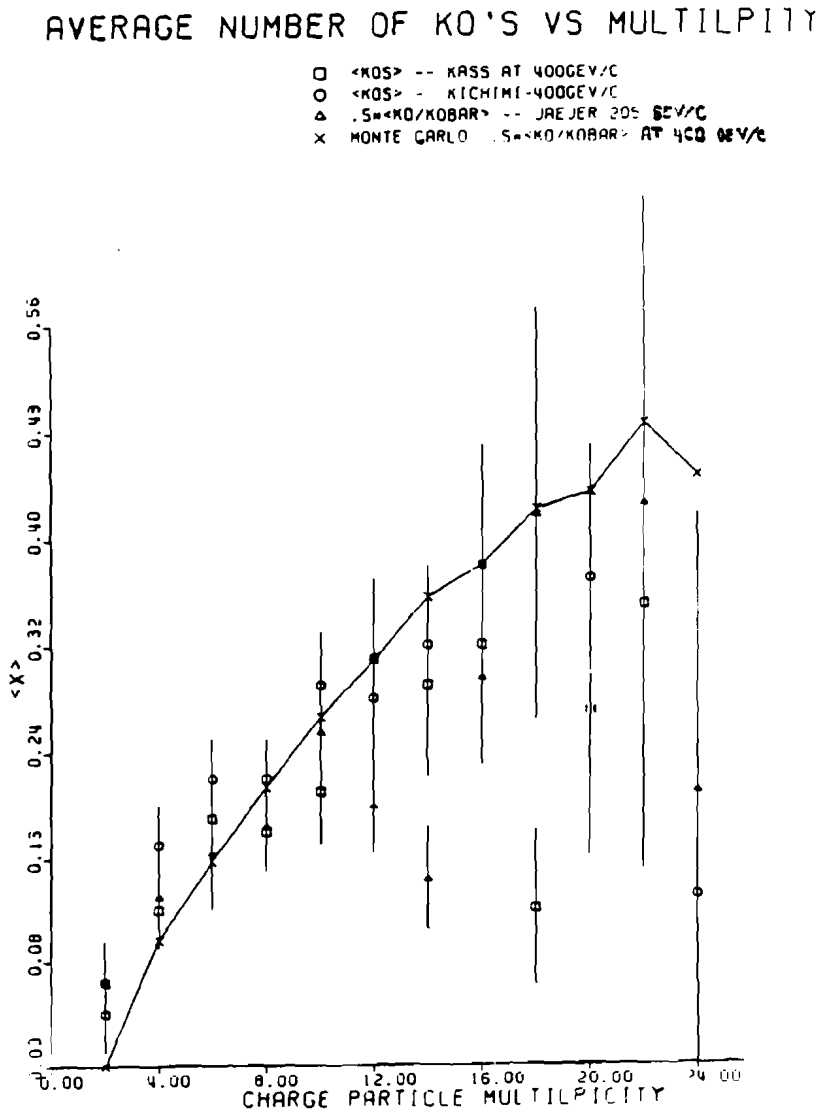

Figure A-4 The total multiplicity for all the Monte Carlo events is shown in the figure below.

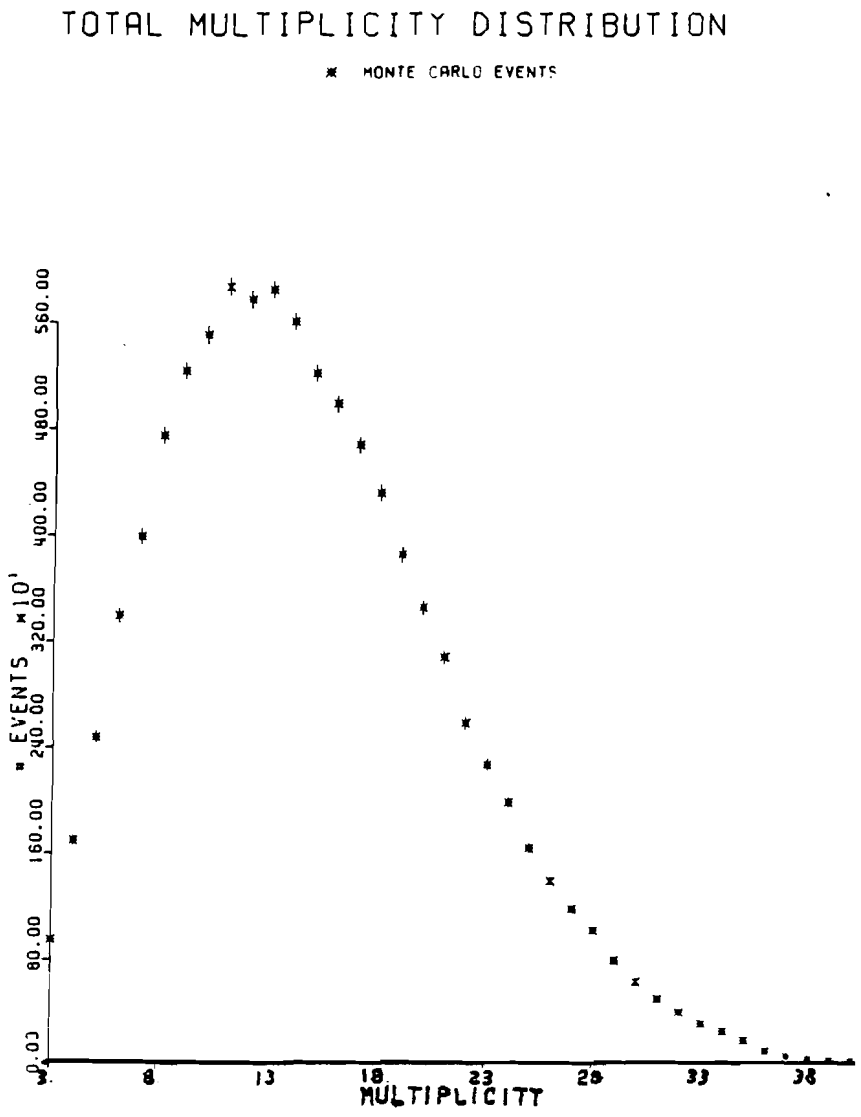

B) Conservation of Energy and Momentum for each Event

The final step is to generate the momentum vector for all the hadrons in such a fashion as to conserve energy and momentum yet still reproduce the experimentally observed kinematic distributions.

The final state hadrons are first given their transverse momentum $\vec{p}_t$. The experimental $|\vec{p}_t|$ distributions for each type of hadron are parameterized;there parameterizations are given in Table A-2. [4,7,8,9,10,11,12] The hadrons are then randomly assigned $|\vec{p}_t|$ values using these parameterizations. Next the transverse momentum vectors are created for each hadron by decomposing $\vec{p}_t$ into two orthogonal compoments,

$$u_i = |\vec{p}_t|_i \cos(\theta_i) \text{ and } v_i = |\vec{p}_t|_i \sin(\theta_i)$$

where θ_i is a random number ranging from zero to 2π generated for each particle i in the final state. Since the p_t for every hadron in a given event is assigned independently of the others, the total transverse momentum will not in general be conserved. To remedy this situation the following transformation is made;

$$u_i \to u_i - (\Sigma_i^n u_i/n) \text{ and } v_i \to v_i - (\Sigma_i^n v_i/n).$$

This procedure guarantees that p_t will now be conserved

for every event. It may be noticed that this transformation process also affects the input p_t distributions. However, due to the steeply falling p_t distributions and the high multiplicities (over 80% of the events have n>9), these corrections are small.† A comparison of the Monte Carlo p_t distributions to the observed experimental data is shown in Figures A-5,6 and 7.

It is important to realize that although this p_t tranformation process produces little change in the overall p_t distribution, it is responsible for kinematic correlations which we find later in our analsis.

The mass and $\vec{p}_t$ is now known for all the hadrons in the generated events. Instead of generating the longitudinal momentum directly we chose to generate the rapidity* instead. This is motivated by the efficient rapidity generation method proposed by Jadack [13]. For a detailed dicussion of this method one should refer to Jadack; however a brief outline is presented below.

The energy and longitudinal momentum constraints

† Lower multiplicity events are of course heavily effected, but this is of little concern since later in the jet analsis it is found that low multiplicity events (<9) rarely satisfy any of our jet triggers.

* $y=(1/2)\log_e[(E+p_l)/(E-p_l)]$

Figure A-5. The transverse momentum distribution for the protons is shown for both the experimental data and Phase Space Monte Carlo events.

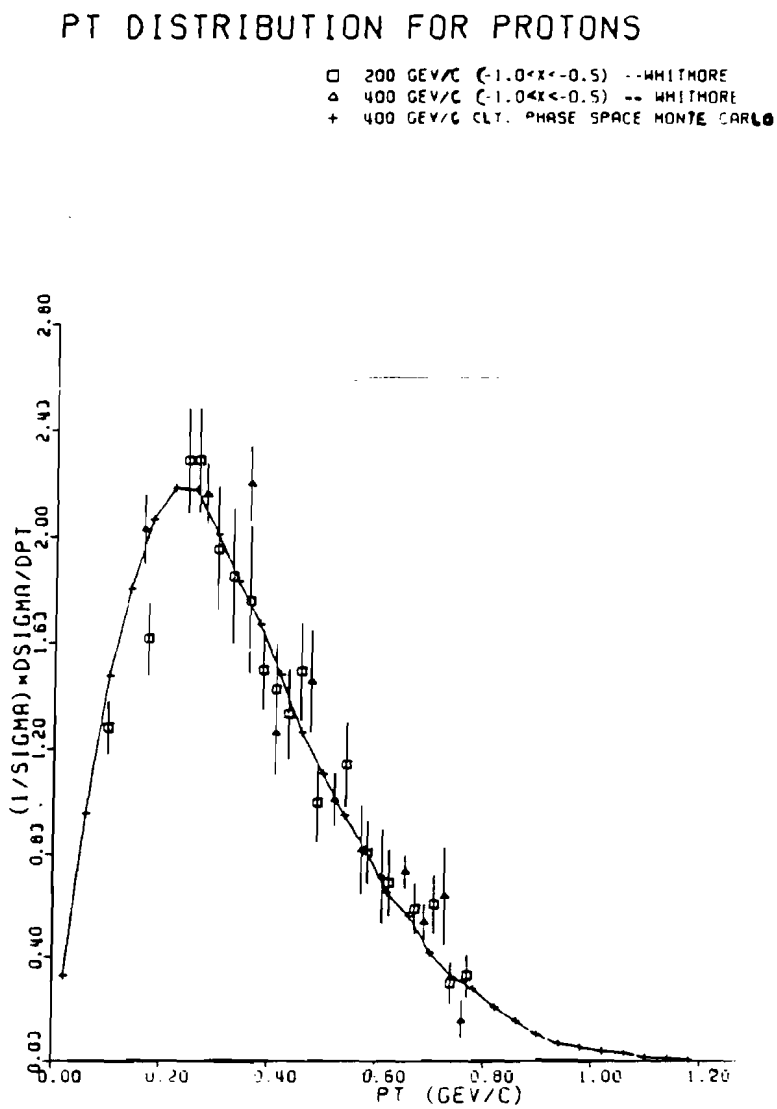

Figure A-6. The transverse momemtum distribution for the pions is shown for both the experimental data and the Phase Space Monte Carlo events.

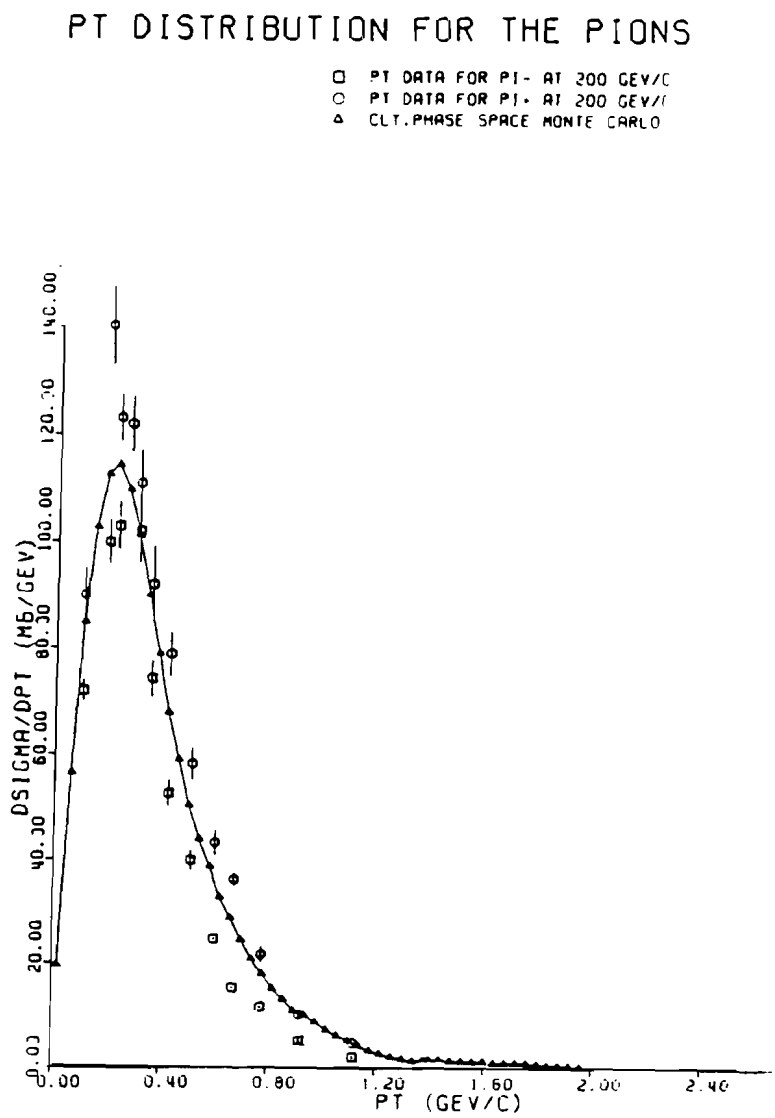

Figure A-7. The transverse momentum distribution for the kaons is shown for both the experimental data and the Phase Space Monte Carlo events.

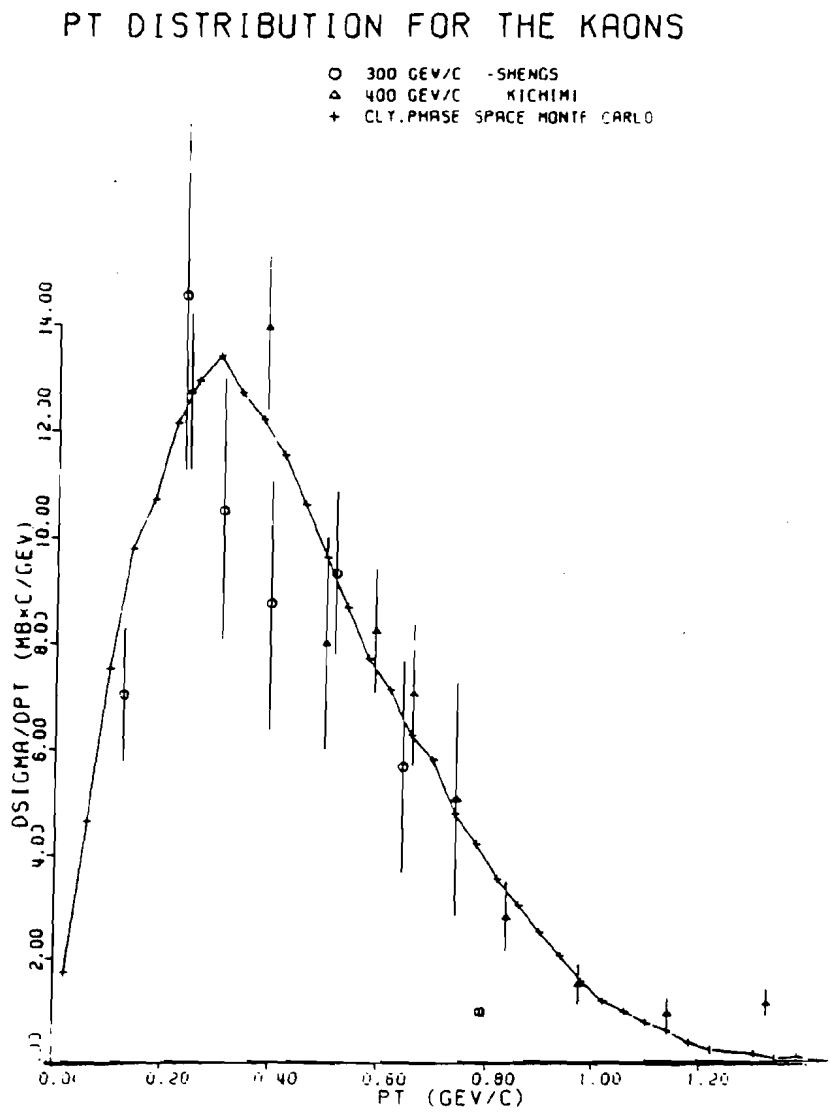

written in terms of rapidity and the transverse mass, m_t, are

$$\left.\begin{array}{l}\Sigma_i^n p_i^L=0\\ \sqrt{s}-\Sigma_i^n E_i=0\end{array}\right\} \mapsto \left\{\begin{array}{ll}\sqrt{s}-\Sigma_i^n m_i^t \exp(-y_i)=0 & \#1\\ \sqrt{s}-\Sigma_i^n m_i^t \exp(+y_i)=0 & \#2\end{array}\right.$$

where $m_t=\sqrt{(m^2+p_t^2)}$

To simply generate n random rapidities y_i such that the above constraints are fullfilled would be too time comsuming. Thus instead, n random variables ξ_i ranging between zero and one are generated and the rapidities are obtained from,

$$y_i=A+B\xi_i,$$

where A and B are constants for each event. By substituting $y_i=A+B\xi_i$ into eqs. #1 and #2 we find,

$$s-\Sigma_i^n m_i^t \exp(-\xi_i B)\Sigma_i^n m_i^t \exp(\xi_i B) = 0 \qquad \#3,$$

$$A-\log_e(\sqrt{s}/\Sigma_i^n m_i^t \exp(\xi_i B))=0 \qquad \#4.$$

B is easily obtained from eq. #3 by a root finding method and A results trivally from eq.#4. Since we have introduced two new constants (A and B) for each event, two ξ_i variables must be assigned, and without loss of generality we can set $\xi_1=0$ and $\xi_n=1$. Hence, for each event the rapidities are obtained by generating n-2 random variables ξ's,

determining A and B, and calculating y_i from $y_i = A + B\xi_i$.

Clearly by controlling the random number distribution function used for the ξ_i variable the rapidity distribution may be manipulated. At Fermilab energies it was found that a flat distribution in ξ produced rapidity distributions that were acceptable as shown in Figures A-8,9,and 10.

The leading particle effect may also be accounted for by requiring that the fast protons recieve the maximum and/or minimum rapidity in a given event (i.e. to be assigned $\xi_1=0$ or $\xi_n=1$). The average number of leading protons in a pp reaction is .9 [14] and is approximately constant independent of multiplicity. Thus our Monte Carlo required that 75%($=.9/\langle p\text{-fast}\rangle_n$) of all events had at least one leading proton. The effect of this kinematic adjustment may be seen in the protons rapidity distribution shown in Figure A-8.

Figure A-8. In this figure the proton's rapidity distribution both with and without the leading particle effect is shown.

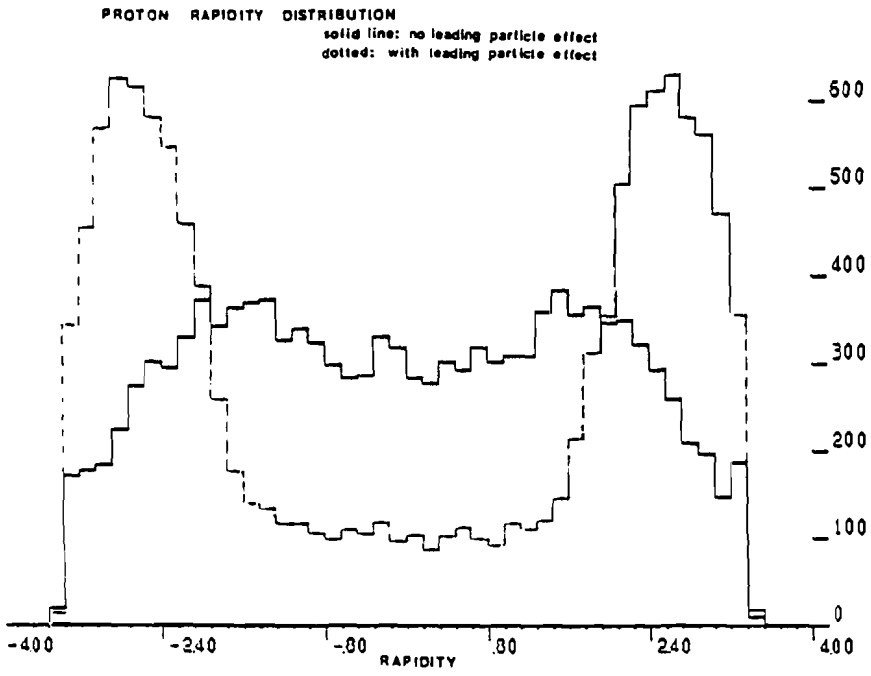

Figure A-9. The experimental pion rapidity distribution is shown along with the corrsponding distribution from the Phase Space Monte Carlo.

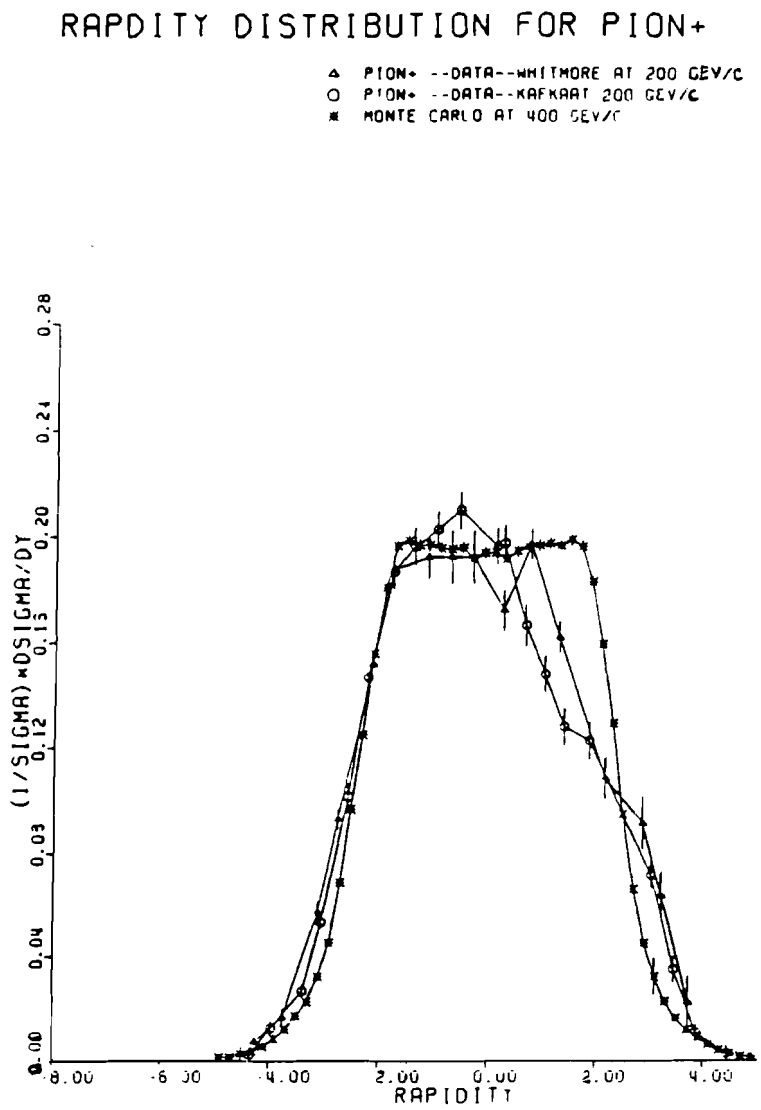

Figure A-10. The experimental kaon rapidity distribution is shown along with the corrsponding distribution from the Phase Space Monte Carlo.

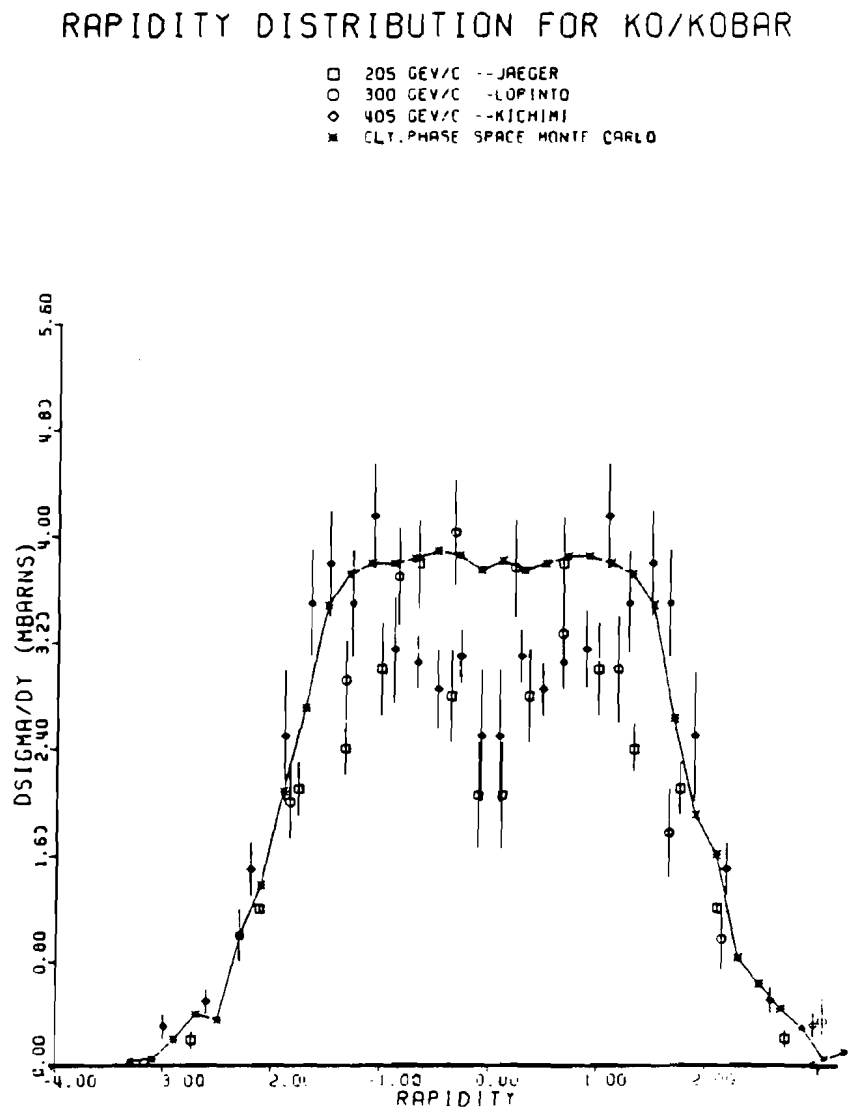

CHAPTER 3

STUDY OF EVENTS SATISFYING A JET TRIGGER

Chapter 2 discussed the Monte Carlo simulation of the low p_t final states in pp inelastic events; this chapter deals with the interpretation of those events which satisfy various trigger requirements. The analysis will consider single and many particle triggers in the centre- of-mass frame and the triggering with a calorimeter in the laboratory frame.

A) Single and Many Particle Triggers in Centre-of-Mass frame.

In the present analysis we have used two fairly typical triggers which illustrate the effects of imposing a "jet trigger" on normal low p_t events. The single particle trigger (S.P.T.) requires that there exist at least one hadron in the event with a polar angle θ greater than 60° and less than 120° and a transverse momentum greater than 1.5 gev/c. The many particle trigger (M.P.T.) demands that the algebraic sum of the p_t for all the hadrons in a solid cone about the momentum vector ($\Delta\theta$=60°, $\Delta\phi$=60°) of the highest p_t hadron be greater than 2.00 gev/c.

Out of one hundred thousand events examined only 182 (0.10%) satisfied the S.P.T. and 901 (0.97%) fullfilled the M.P.T. conditions. A comparison between the total multiplicity distributions of all events and the triggered events is shown in Figure B-1. This figure illustrates probably the most important result of our analysis; it shows that the probability of satisfying the jet triggers increases greatly as the multiplicity goes up. This is greatest for the M.P.T., but even for the S.P.T. the most probable number of hadrons in a triggered event is 18 as compared to 15.2 for all events. The average multiplicities are 27.8 and 20.6 for the M.P.T. and S.P.T. respectively.

One might surmise that there is a natural tendency towards higher and higher multiplicities as the p_t triggering level is increased. This is indeed correct as can be verified in the scatterplot of Figure B-2, where the multiplicity is plotted against the p_t triggering level for the M.P.T.. From this scatterplot one finds that the average multiplicity increases approximately linearly with the p_t level, $\langle n \rangle = 4.3\ p_t + 14$ for $p_t > 2.00$ gev/c. Its clear that it is much more probable for the higher p_t requirements to be met more frequently by a great number of low p_t hadrons than by a few high p_t hadrons.

Figure B-1. The total multiplicity distribution is shown for all of the Monte Carlo events and for those events which satisfy the Many Particle Trigger and the Single Particle Trigger.

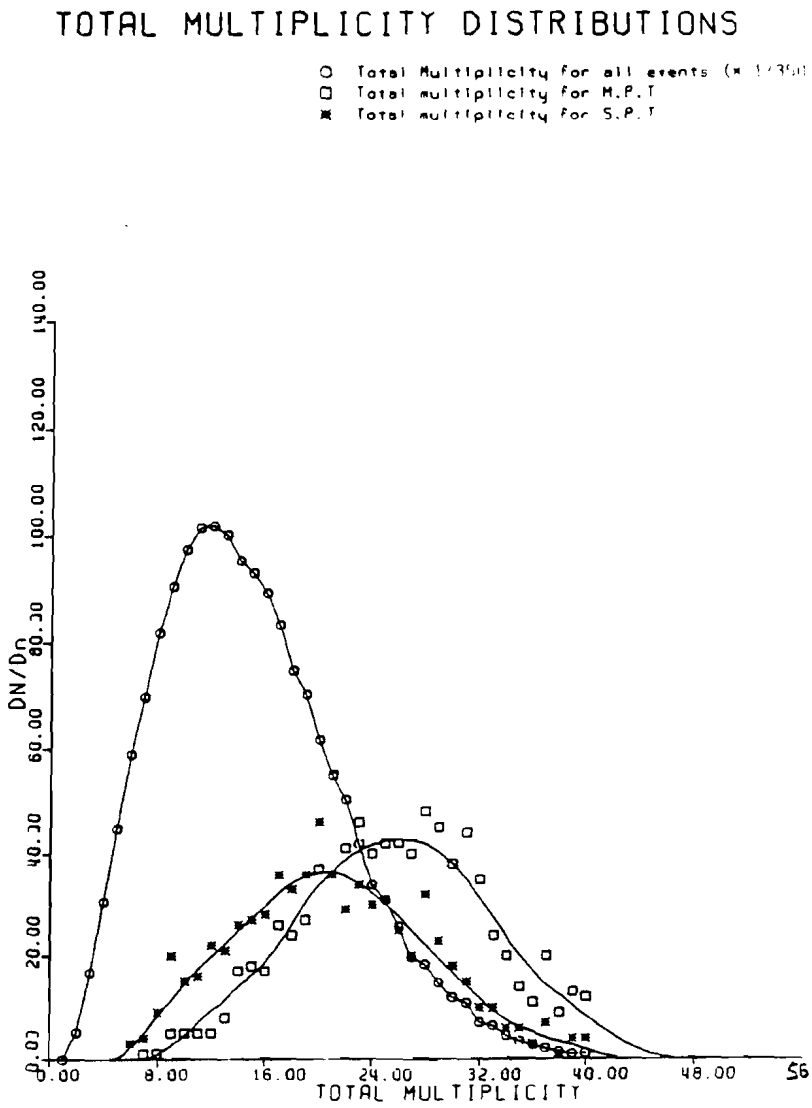

Figure B-2. This figure is a scatterplot of the total multiplicity and the transverse momentum triggering level for the many particle trigger.

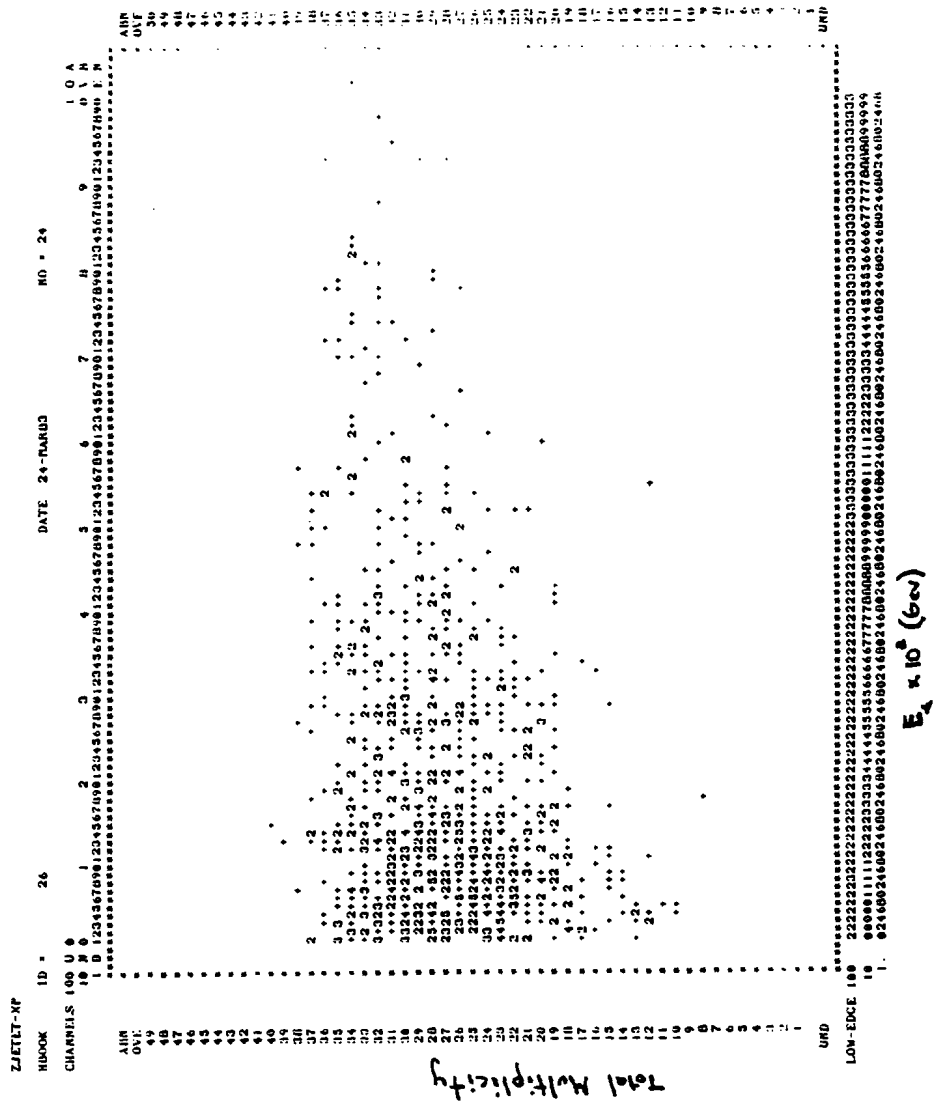

It is of interest to determine how the jet-like structure of an event changes as the multiplicity increases. Thus a parameter characterizing jet structure is needed; one commonly used variable is planarity P, defined by P=(A-B)/(A+B), where A and B are the eigenvalues of the momentum tensor P_{xz},

$$P_{xz} = \begin{pmatrix} \Sigma(p_x^i)^2 & \Sigma p_x^i p_z^i \\ \Sigma p_x^i p_z^i & \Sigma(p_z^i)^2 \end{pmatrix},$$

where X and Z are the coordinates of the transverse plane. The sum is over all the hadrons in the event. P approaches one as the event becomes pencil-like, and tends towards zero for istropic events.

One might expect that the planarity distribution for triggered events would be shifted towards unity as compared to all events, because high p_t events tend to be more planar. As Figure B-3 shows however, this is not the case; there appears to be very little change in the planarity distribution from all to triggered events. The explanation for this effect is found by studying the scatterplot of multiplicity against the planarity (Figure B-4) for all events. The most striking feature is that very high planarity (>.9) is obtainable only with very low multiplity (<4) and the planarity then decreases very rapidly with increasing

Figure B-3. In this figure the planarity distributions for all Monte Carlo events and for the "Many Particle Trigger" is shown.

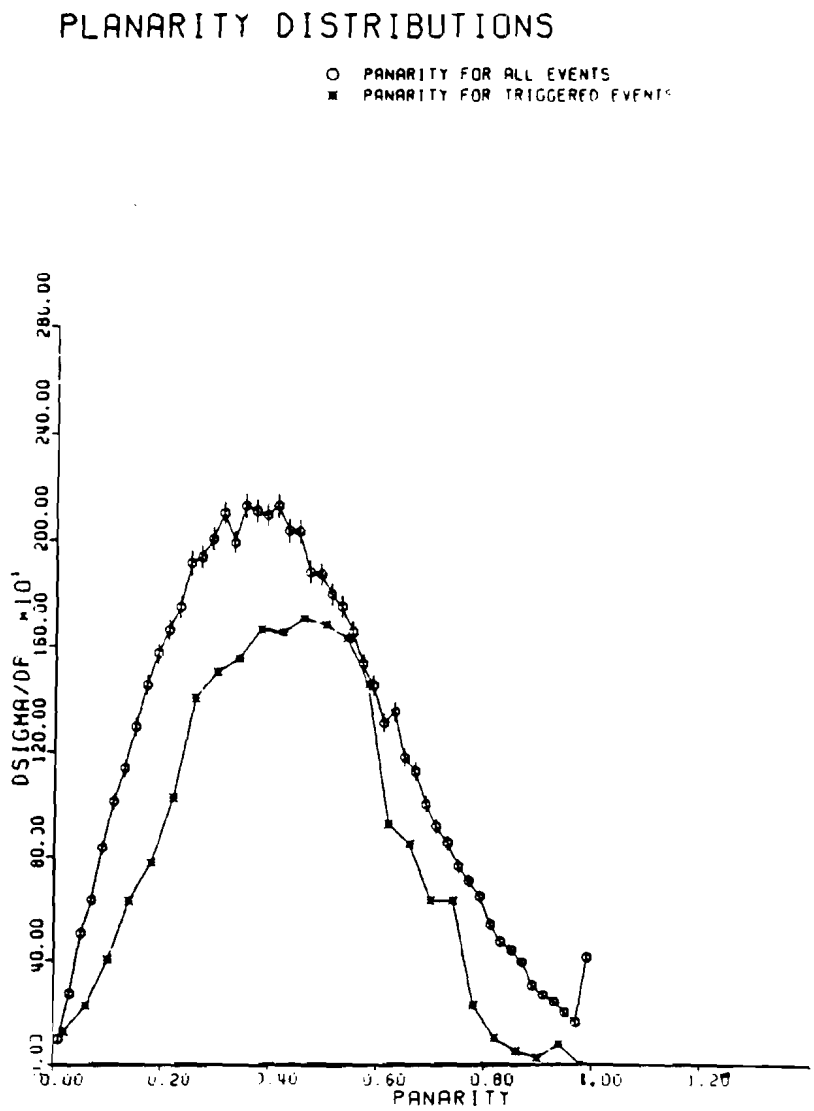

Figure B-4. A scatterplot of the multiplicity and planarity for all the Monte Carlo events is shown.

MULT-PLANE XSTEP= 4 YSTEP= 1 UNDER/OVERFLOW=<

Multiplicity	0<				20*				40*						60*				80*				100*	
	<	*	*	*	*	*	*	*	*	*	*	*	*	*	*	*	*	*	*	*	*	*	*	*
39>	.	.		.	1			1		1														
38*	.	1	.	1	1	1		1			1	.	.	.	.	.	.							
37*	.	1	3	4	3	4	4	2	.	.	1				2	.		1						
36*	1	3	5	1	8	6	5	3	6	2	3	2	2	6	3	1	.							
35*	1	2	8	8	9	7	10	12	9	6	2	8	2	1	3	3		1						
34*	3	7	15	13	12	14	9	12	14	15	11	4	3	5	4	2	.							
33*	2	4	11	11	9	17	18	17	14	17	9	8	11	8	3	6	2	.		1	.			
32*	1	9	15	10	21	24	18	24	20	11	27	20	9	9	7		1	2	2		.			
31*	1	11	17	15	33	32	33	31	26	28	23	26	16	13	15	7	4	1	1		.			
30*	4	14	25	40	36	36	28	41	34	26	29	31	15	27	10	9	4	4	1		.			
29*	8	16	19	41	45	34	60	52	42	37	47	35	37	18	14	14	4	1	3	2	.			
28*	4	19	20	33	46	53	58	69	55	46	49	40	29	24	30	13	8	7	3	.	.			
27*	3	21	25	44	64	74	77	57	65	64	65	50	43	52	23	19	13	4	3		.			
26*	7	22	39	50	68	73	78	83	67	70	78	63	56	43	20	15	13	6	9	4	1	.		
25*	4	25	44	63	99	88	109	75	83	99	72	84	62	61	47	36	21	13	4	2	1	1		
24*	13	32	40	59	73	93	107	99	105	104	101	98	60	64	45	33	24	17	6	2	1	.		
23*	8	35	50	66	89	105	104	127	119	108	109	123	92	73	63	40	34	24	10	3	2	1		
22*	11	37	67	85	114	130	125	131	146	153	143	139	122	93	69	74	50	27	17	9	3		1	
21*	15	37	79	103	136	126	137	121	135	148	148	132	132	104	102	61	51	28	25	15	4			
20*	18	43	75	98	120	149	158	174	168	213	174	170	154	113	106	89	68	48	25	17	2	1		
19*	20	64	72	98	126	174	159	181	209	179	186	177	163	146	133	92	85	59	45	11	7	1		1
18*	29	51	92	118	137	183	186	221	221	180	212	192	191	178	142	120	82	84	47	45	12	4	4	1
17*	17	66	90	109	143	193	181	228	223	233	243	226	225	167	165	133	107	103	70	35	24	10	3	
16*	12	69	80	127	132	191	213	222	252	234	251	248	215	224	171	153	131	112	67	55	32	15	6	
15*	22	55	84	133	193	213	216	202	231	245	227	258	219	236	212	182	156	125	89	54	48	26	5	1
14*	15	51	95	111	166	169	216	219	242	262	255	263	249	244	223	172	173	124	118	72	57	33	12	1
13*	9	58	87	117	156	178	196	223	223	244	263	247	246	256	238	212	205	149	112	94	53	33	21	5
12*	16	54	85	114	147	173	187	207	224	239	231	254	261	262	242	208	210	173	146	121	78	37	22	7	1
11*	15	37	69	107	139	152	192	215	224	218	237	242	215	267	240	222	225	204	164	126	101	60	39	17	
10*	17	57	79	100	110	156	161	199	204	196	245	218	233	226	270	235	203	174	156	148	130	80	60	17	2
9*	20	27	47	81	100	133	142	137	164	190	191	179	200	211	222	224	222	193	183	121	113	85	63	19	2
8*	8	31	43	63	76	84	108	129	153	145	160	196	177	180	202	199	181	171	182	184	149	113	87	44	8
7*	3	19	34	46	64	69	78	109	94	123	107	118	127	178	165	172	140	169	156	139	138	101	103	76	23
6*	5	12	23	39	45	44	54	55	83	80	118	88	117	98	126	117	130	138	151	117	114	108	106	91	38
5*	4	10	10	15	34	29	37	34	50	65	56	67	69	69	84	81	88	93	123	91	109	99	109	93	66
4*	1	5	4	6	14	15	15	19	32	21	31	34	30	46	46	61	48	56	64	73	87	81	97	122	104
3*	.	1	1	.	6	7	7	5	8	5	12	5	14	10	11	15	13	25	28	31	38	47	61	71	183
2*		.	.	.				.		.														19	185

Planarity ($\times 10^3$)

multiplicity. Since the trigger requirement chooses preferentially high multiplicity events and therefore low planarities, the net result is very little change in the planarity distribution for triggered events as was seen in Figure B-3.

As mentioned earlier there is an induced p_t-ø correlation in the simulation procedure; it's effect may be seen in the plot of Δø for all hadrons in an event which satisfies the S.P.T. (Figure B-5). Δø is the azimuthal angle in the transverse plane measured from the p_t vector of the highest p_t particle to the hadron in question. Figure B-5 shows that there tends to be more particles on the opposite side (Δø>90°). This effect is due to the rotation of the lower p_t from the highest, occuring in the process of balancing transverse momentum. If the p_t triggering level is increased then one observes an increase in the slope of the Δø distribution.

Our method of balancing momentum also introduces small rapidity and p_t correlations as shown in Figures B-6 and B-7. Figure B-6 is a plot of the ratio of the normalized away side p_t distribution to the input (all events) p_t distributions for the S.P.T.; this curve shows that the away side p_t distribution is broader for triggered events.

Figure B-5. In this figure the azimuthal angle phi for every particle relative to the highest transverse momentum paricle is plotted.

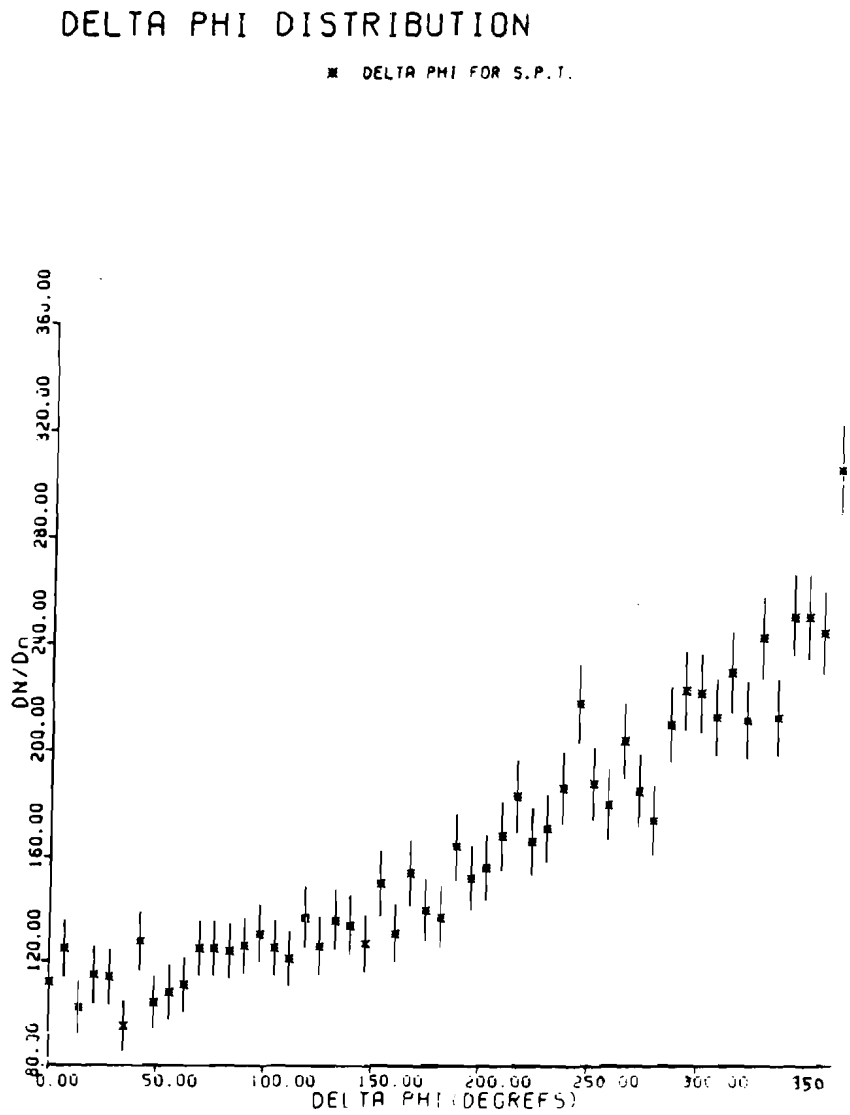

Figure B-6. The ratio of the normalized p_t distributions for the away side and the Monte Carlo is shown below.

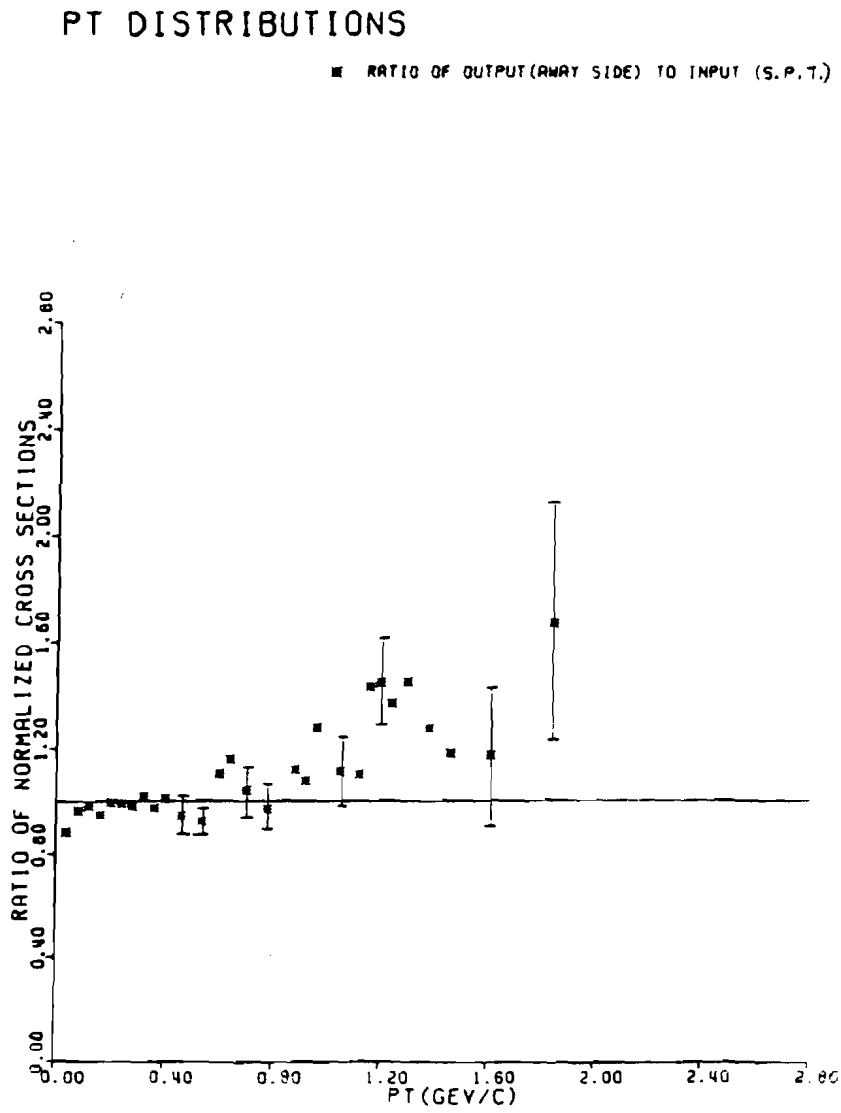

Simarily Figure B-7 is a plot of the ratio of the normalized away side rapidity distribution to the input rapidity distribution; this curve shows that the away side rapidity distribution is narrower for the triggered events, that is there is a depletion of particles with high rapidity values and a enhancement of particles in the central region.

The importance of the three correlations mentioned above should be stressed. They are all due to our method of balancing momentum and energy. However, similar correlations have been found in actual experiments under similar trigger conditions [17]. Our analysis shows that at least part of the correlations maybe due to "trivial" kinematic effects, and cannot be considered as evidence for jet structure.

B) Triggering with a Calorimeter in the Laboratory Frame

One of the motivations of this analysis was to understand the effect of imposing triggers used in the E609 experiment on the generated low p_t events. This experiment [18] uses a multiple-segmented calorimeter (shown in Figure B-8) to trigger on "jet events" by requiring that the algebraic sum of the $E_t(p_t)$ deposited in a particular

Figure B-7. The ratio of the normalized rapidity distributions for the away side and the input Monte Carlo is shown below.

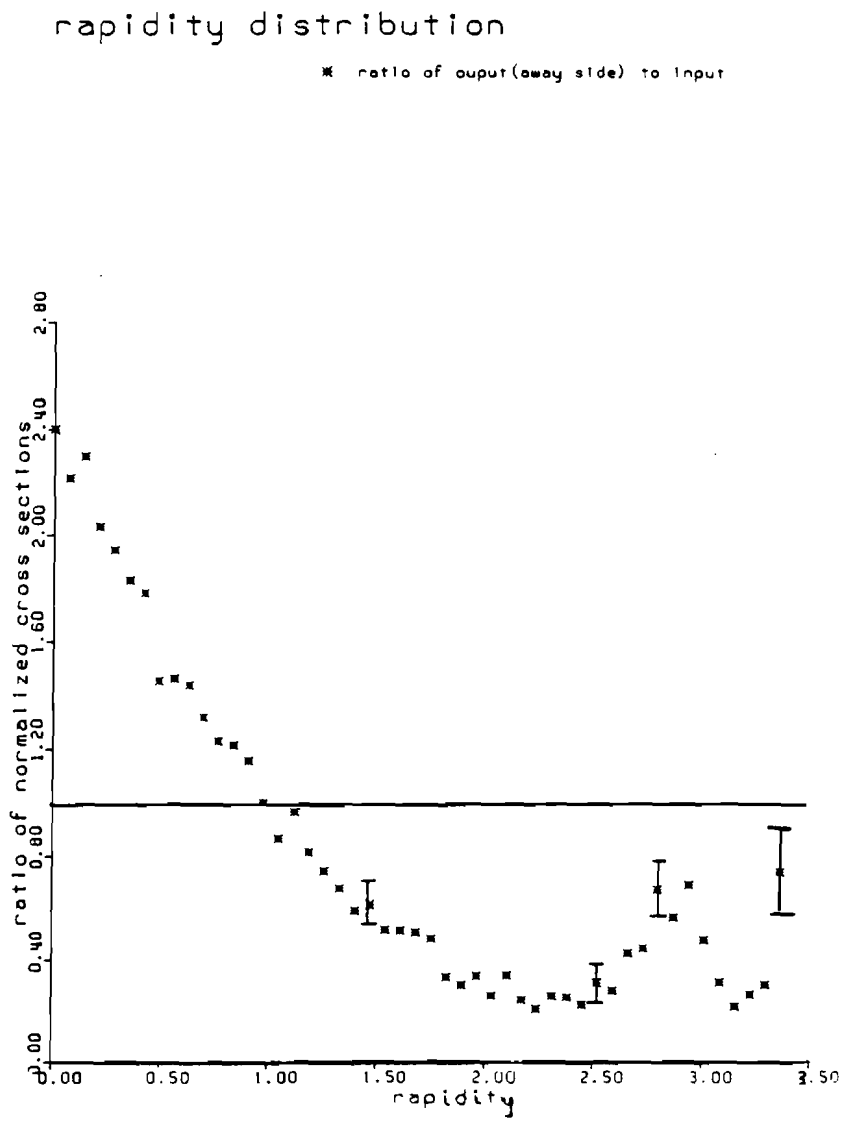

Figure B-8 An oblique view of the calorimeter showing it's layered structure and its postion relative to the target is sketched below.

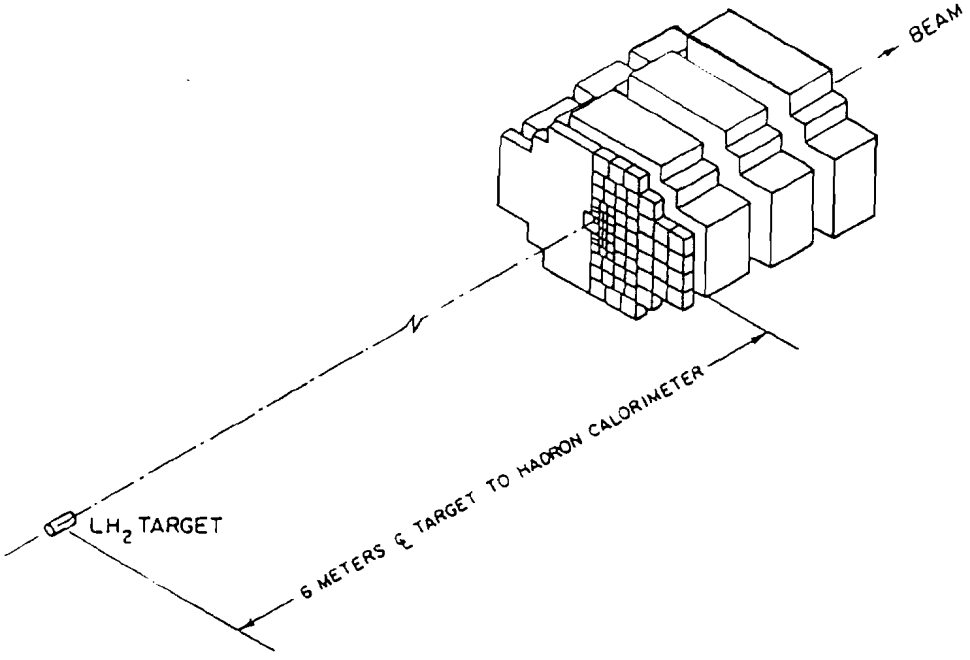

combination of the segments be greater than some E_t threshold level; however, for simplicity the analysis here will deal with three basic trigger configurations, the Global,Double Arm, and Single Arm triggers as shown in Figure B-9.

The Global trigger which covers approximately 8 srad. (in the centre-of- mass) was used with a 7.00 gev/c triggering threshold. Of 100000 events examined 1220 (1.27%) satisfied the triggering requirements. An overall evaluation of these globally triggered events may be seen by comparing the total multiplicity distribution of the input (all events) to the output (triggered events) as shown in Figure B-10. As found in the centre-of-mass analysis the total multiplicity distribution of the triggered events is shifted upwards, in this case the average multiplicity changes from 15.2 for all events to 31.5 for the triggered events.[τ] Simarily the average p_t increases from an input value of $\langle p_t \rangle = .36$ gev to $\langle p_t \rangle = .41$ gev for the triggered events. The planarity distributions (see Figure B-11) shows a small decrease in the average planarity from the input events to the output, the average changing from .41 to .318. To examine the planarity further a plot of the average planarity .vs E_t is shown in Figure B-12;it is clear that there appears to be

[τ] The multiplicity that the caliormeter observe's would be (due to the limiting geometry) approximately 60% of the original Monte Carlo multiplicity.

Figure B-9. The figure below is a cross-sectional view of the calorimeter. Various triggers may be formed by combinations of the segments, the Double Arm trigger is shown outlined and the shaded region shows the Single Arm trigger.

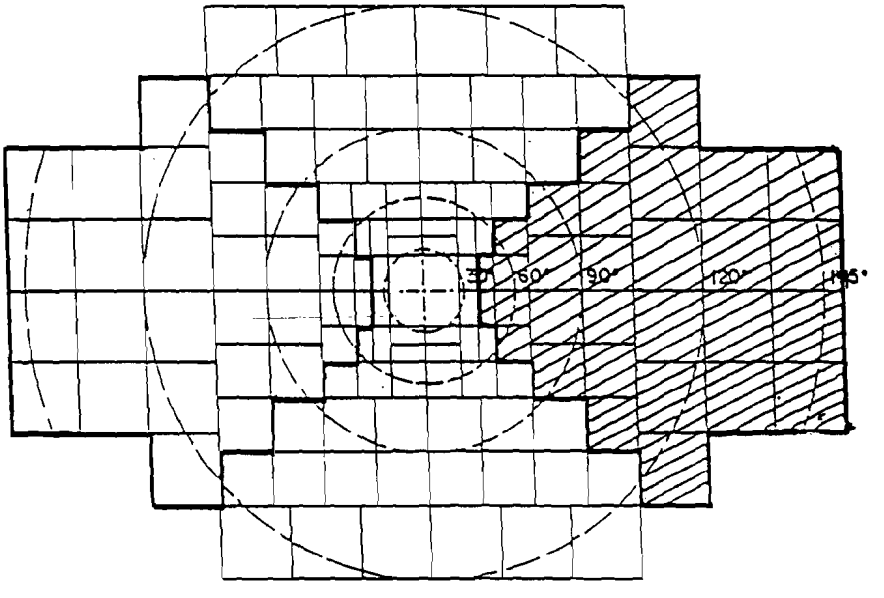

Figure B-10. In this figure the total multiplicity distributions for the Monte Carlo events and for those events satisfying the global trigger is shown.

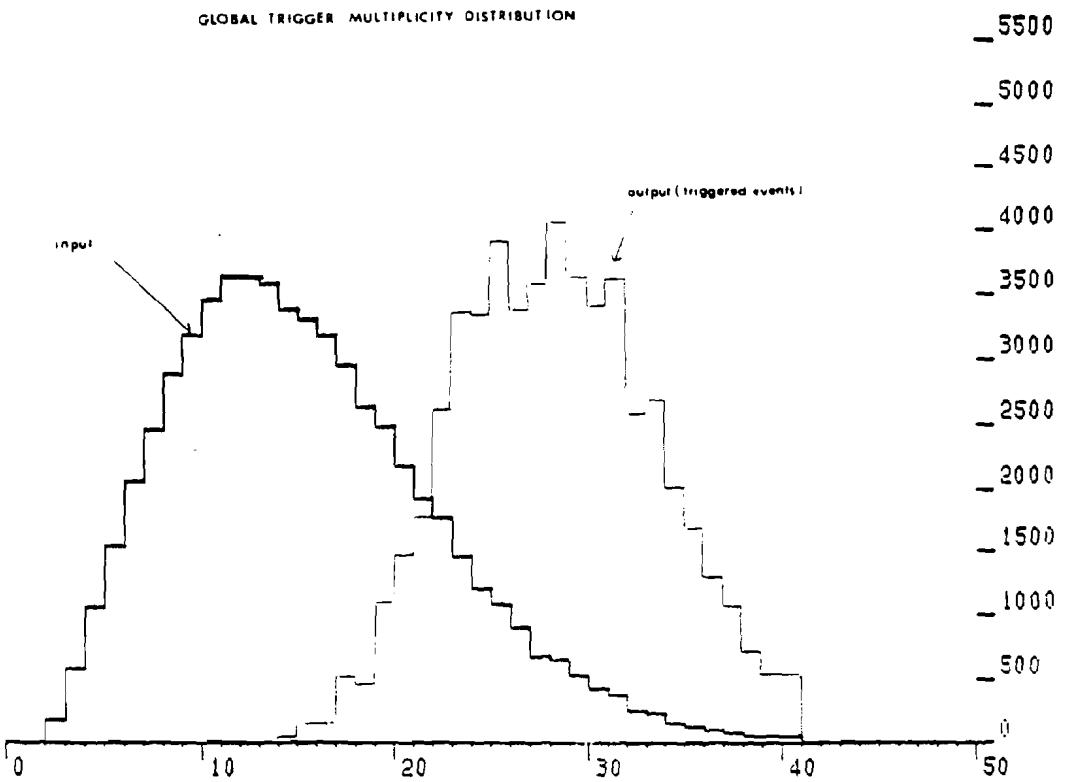

Figure B-11. In this figure the planarity distributions for the globally triggered events and the Monte Carlo events is shown.

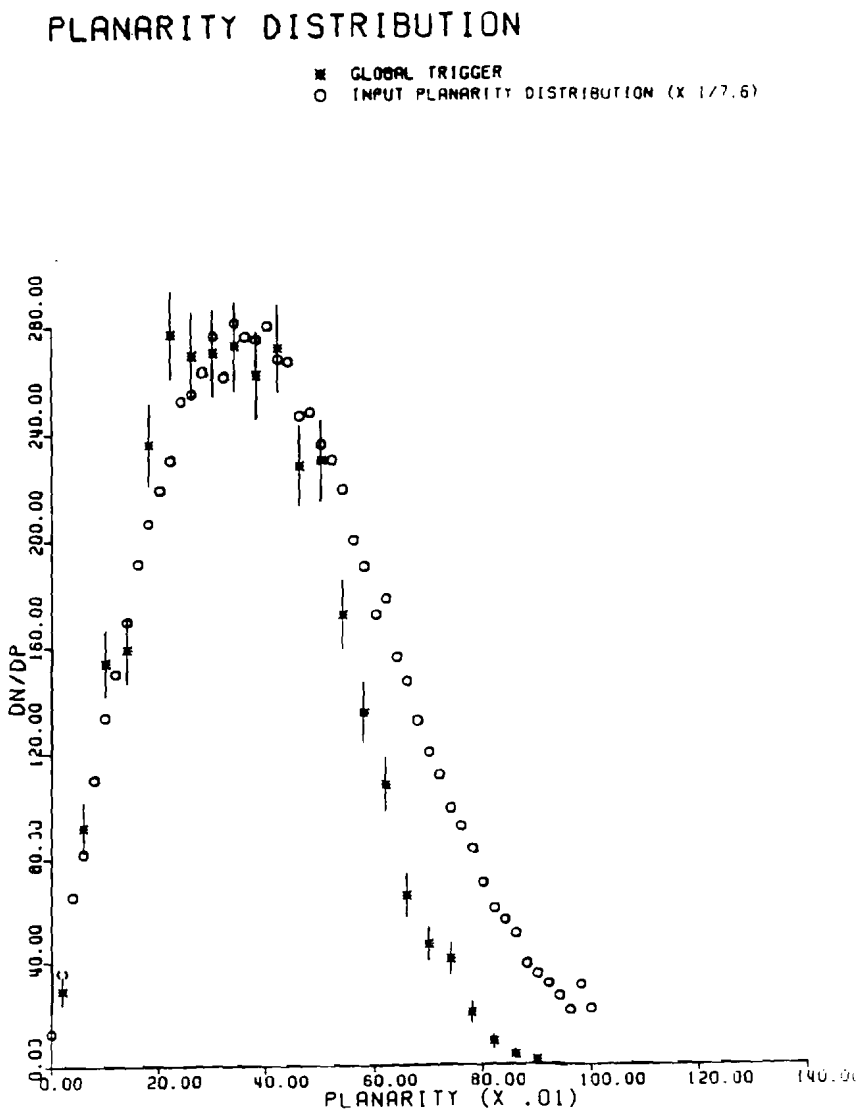

Figure B-12. The average planarity for globally triggered events is shown here as a function of the transverse energy.

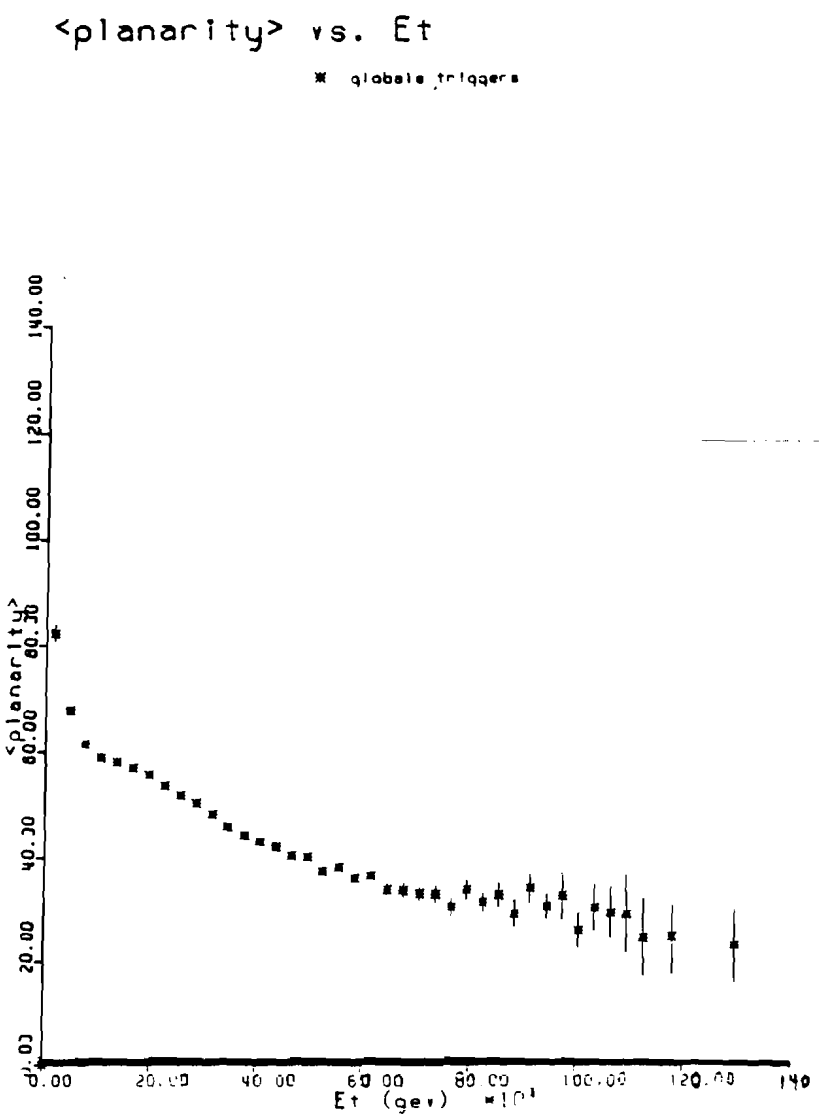

a slight decline in planarity as the E_t in the triggering region (ie. the entire calorimeter here) increases.

A comparison of this data with that of Fermilab experiment E557 [19] shows that although at E_t=7.00 gev/c <planarity> is approximately the same as the observed data, at higher E_t thresholds (E_t> 10.0 gev/c) the actual data has planarity values a factor of 1.4 greater than this phase space data. One may then infer that the real data has somewhat more coplanarity than the phase space events.

In Figure B-13 the triggering rate is shown as a function of the transverse energy for the global trigger. The data may be fitted by the function $\frac{d\sigma}{dn}=A\ \exp(-\alpha E_t)$ with α=.84, comparing with similar data from the E557 experiment reveals (α=.84.) excellant agreement.

The Single and Double arm triggers shown in Figure B-9 cover 1.4 and 2.8 sradians (centre-of-mass) and with triggering levels of 2.00 gev/c and 4.00 gev/c respectively, .94% and .40% of all the inelastic events satisfy the single and double arm trigger conditions. An examination of the total multiplicity distribution for events satisfying each trigger condition yields the mean multiplicity for the double arm trigger <n>= 30.4 and for the single arm trigger

Figure B-13. In this figure the triggering rate as a function of the transverse energy is shown for the global,double arm and single arm triggers.

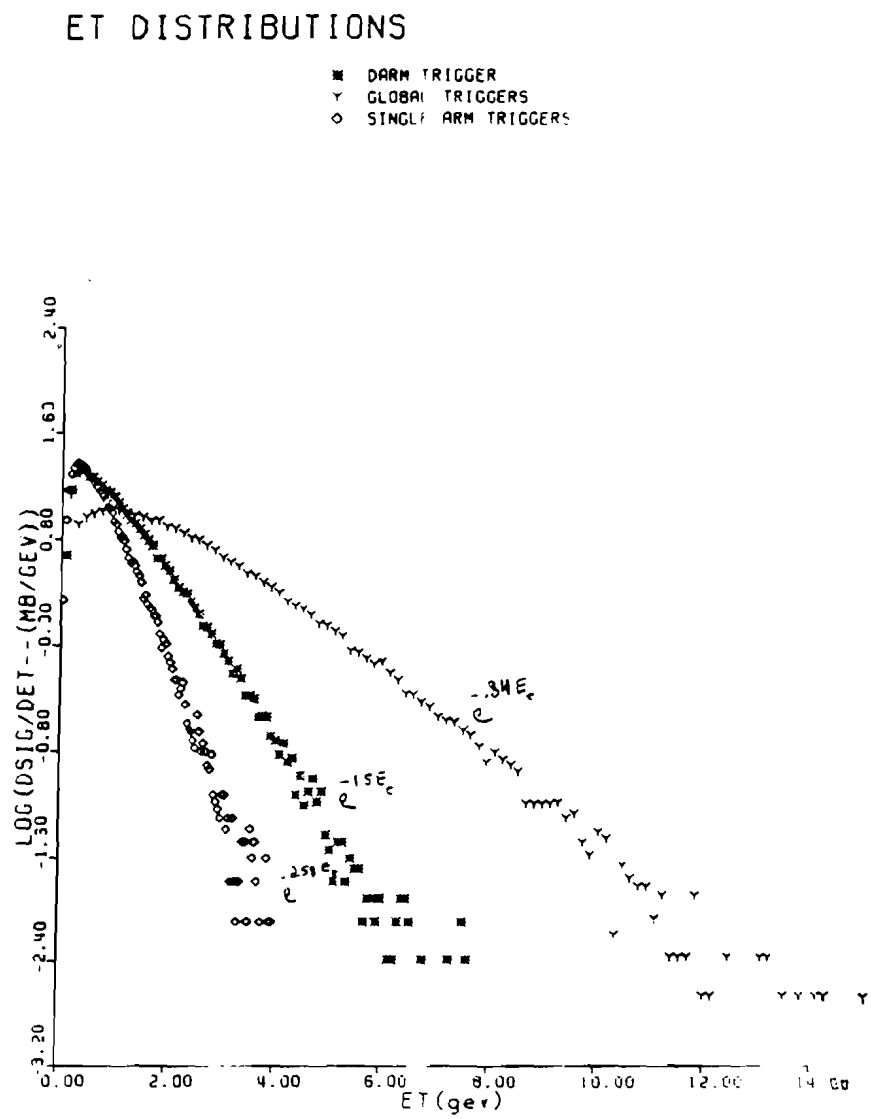

$\langle n \rangle = 27.8$. The mean transverse momentum for for the triggered events was quite similar to the global case, $\langle p_t \rangle = .406$ gev/c for the single arm and $\langle p_t \rangle = .416$ for the double arm trigger. Both the triggers however give planarity distributions that within statistics seem to be similar; $\langle \text{planarity} \rangle \approx .45$ noticably higher than the global events and slightly higher than the unbaised (input) events. The E_t dependence of the cross section for each trigger,shown in Figure B-13, shows that α increases as the triggering solid angle decreases. An exponential fit to the data results in $\alpha = 1.51$ for the Double arm trigger and $\alpha = 2.58$ for the Single arm trigger; this is also the trend that is found in the E557 experimental data. Another interesting comparison to the known experimental data [19] is the E_t dependence of the mean planarity; it is found that within statistics the dependence of both triggers is identical to the global case which is quite contrary to the published data showing that as the triggering solid angle decreases the $\langle \text{planarity} \rangle$ for any fixed E_t increases.

Of concern also is how the transverse momentum is balanced in these triggered events. The Single arm trigger may or may not have the majority of the balancing E_t in the symmeterical region on the away side. Figure B-14 shows a scatterplot of the triggering E_t and the E_t in the

Figure B-14. The balancing transverse momemtum for the single arm triggers is illustrated by the scatterplot of the triggering side E_t and the away side E_t.

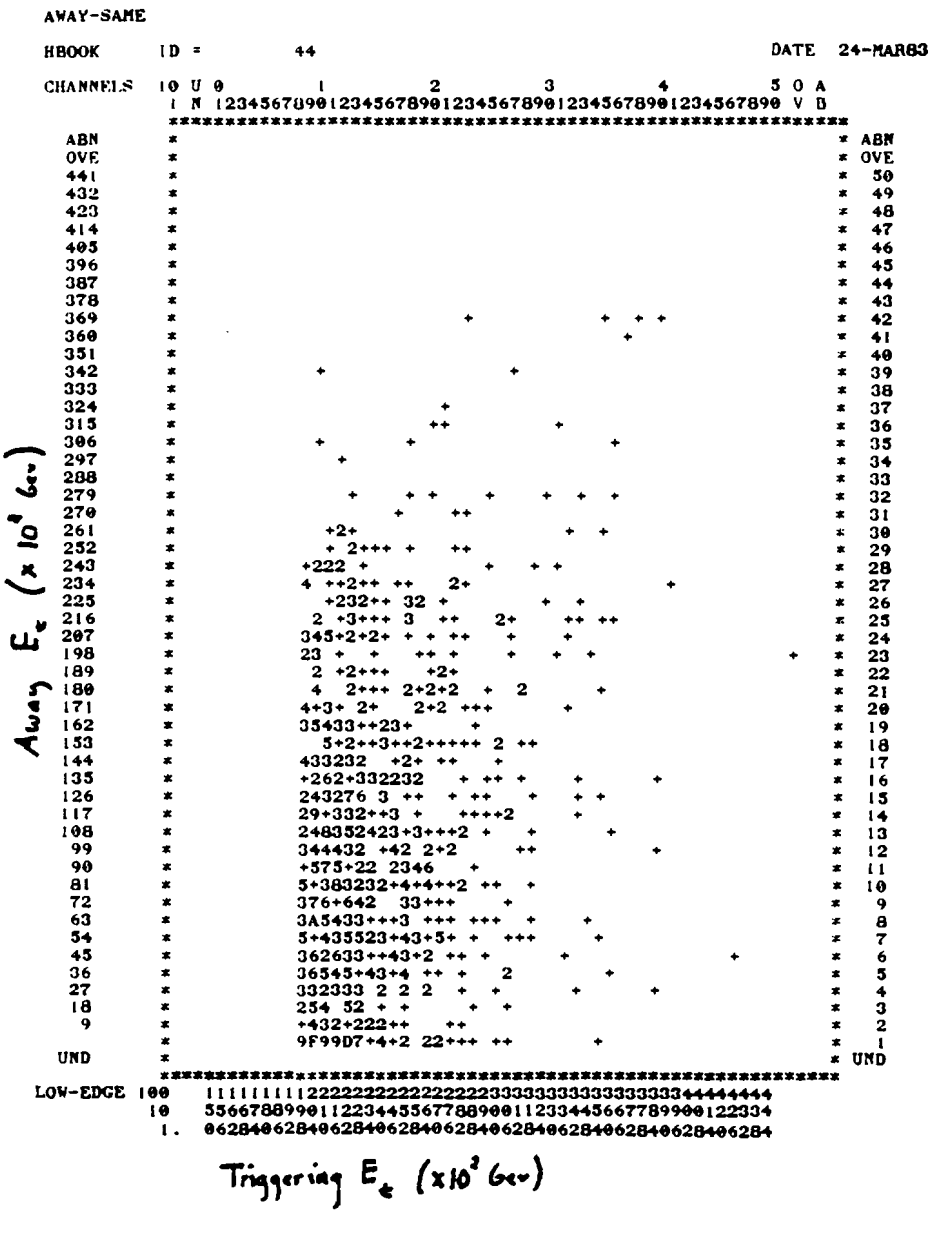

symmeterical away side region. It is evident from the scatterplot that the majority of the balancing E_t is not localized, but is spread out on the away side. (In fact 9.0% of all the single arm triggers have nothing in the symmetrical region on the away side, the balancing E_t being outside this area or perhaps not in the calorimeter at all.) This obversation is a simple consequence of our global p_t balancing procedure in the generation process.

CHAPTER 4

CONCLUSIONS

We have studied the properties of typical inelastic final states in pp collisions at p_{lab}=400 gev/c under triggering conditions similar to those used in actual jet experiments. The events were generated with a Monte Carlo method by using as input distributions the experimentally observed charged multiplicity and inclusive momentum distributions. All the events were required to conserve four-momemtum and some other quantum numbers; momentum conservation was imposed in a minimal way by sharing the unbalanced transverse momentum equally amoung all the hadrons. We have not included the effects of resonances or any other dynamic correlations.

The generated events were studied with four high transverse momentum triggers: a single particle, a single arm,a double arm and a global trigger. In each case it was found that the accepted events had multiplicities much higher than the nontriggered events, and that the multiplicity increased significantly with increasing E_t threshold.

With the single particle trigger we find that the

accepted events show correlations (rapidity, p_t, and azimuthal angle) which are somewhat weaker but qualitatively similar to those observed in past experiments. It thus appears that it is important to try to separate these effects from true dynamical correlations before interpreting the results of these experiments.

When triggering in groups of hadrons, we find that the transverse energy spectrum for each type of trigger (single, double and global) is similar to that in actual data. The mean planarity for globally triggered events was found to be about 25% lower than that observed experimentally, and decreases with increasing E_t in slight disagreement with the data. All of these results can be understood as a consequence of the fact that in our Monte Carlo a high E_t trigger threshold can be satisfied only with very high multiplicity events.

It seems clear that even though some experimentally observed correlations may be explained by "trivial" kinematic effects and that the actual high transverse energy events has a similar E_t dependence, the obsversed data has a higher degree of coplanarity than what is dictated by pure phase space considerations.

REFERENCES

1. R.Moller,Nuclear Physics 1374,145,(1974).

2. Z.Koba,H.B.Nielsen and P.Olesen, Nucl. Phys. B40 (1972) 317.

3. A.J. Buras, et al., Physics Letters 47B,3,251,(1973).

4. M. Antinucci, et al. Nueovo Cimento,6,4,121 (1973). (We have taken the liberty of changing some the the numbers given in this reference so that the results are consistent with charge conservation.)

5. A. Sheng, et al., Physical Review D, 11,7,1733,(1973).

6. R.D. Kass, et al., Physical Review D,20 3,605,(1979).

7. J. Whitmore, Physical Reports,10C,5,274,(1979).

8. T. Kafka, et al., Physical Review D,16,5,1261,(1977).

9. J. W. Cronin et al., Physical Review Letters,31,1420,(1979).

10. H. Kichimi, et al., Physical Review D,22,1,37,(1979).

11. F. Lopinto, et al., Physical Review D,22,3,573,(1980).

12. K. Jaeger, et al., Physical Review D,11,9,2405,(1975).

13. S. Jadach, Nuclear Letters,47B,3,251,(1973).

14. J. Whitmore, Physical Reports, 27C,5,188,(1976).

15. F. T. Doa, et al., Physical Review D,10,11,3588,(1974).

16. F. T. Doa, et al., Physical Review Letter,

30,22,1151,(1973).

17. M.G. Albrow et al., Nucl. Physics B145 (1978) 305.

18. W. Selove et al., prelimarly report given at the 21st International Conference on High Energy Physics at Paris France.

19. B. Brown, et al., Physical Review Letters, 49,10,711,(1982).